Solar Energy 171 (2018) 804–810

Contents lists available at ScienceDirect

Solar Energy

journal homepage: www.elsevier.com/locate/solener

Modified vacuum tubes for overheating limitation of solar collectors: A dynamical modeling approach

Luis E. Juanicó

Instituto Andino-Patagónico de Tecnologías Biológicas y Geoambientales (IPATEC), CONICET and National University of Comahue, 8400 Bariloche, R. Negro, Argentina

ARTICLE INFO

Keywords:
Thermal-solar modeling
Dynamical modeling
Vacuum-tube solar collectors
Solar collector overheating

ABSTRACT

In this paper are presented two designs of vacuum tubes designed to avoid the overheating of solar collectors. As we discuss, this behavior must be studied by considering the collector's nonlinear dynamic, which is numerically studied by developing a solar-thermal modeling based on a fourth-order approximation for the efficiency function. In this way, the two main heat-losses mechanisms involved can be simulated and so, two kinds of modified vacuum tubes are studied: (a) by increasing its heat convection coefficient and (b) by increasing its infrared emissivity. Therefore, we have calculated their modified efficiencies in order to get a non-overheating collector, in which the maximum design temperature is always kept below 111 °C (for water-in-glass tubes) or 131 °C (for heat-pipe tubes). Then, we have studied the performance of these collectors when they work on low temperatures, showing that the first design of modified vacuum tubes (increasing the convection heat losses) penalizes the collector's performance up to 26%, meanwhile the second design (increasing the infrared heat losses) does not change the collector's performance. Therefore, a new collector based on these tubes could improve its performance on cloudy days by using a greater number of vacuum tubes. In this way, we found that by using 50 standard tubes (instead of 20 tubes) a solar collector based on a 200-l water tank could satisfy the daily household demand of hot water (200 kg@45 °C) even during cloudy days.

1. Introduction

The vacuum-tube solar collectors is a mature technology for providing sanitary hot water demand (SHWD). Comparing to the flat solar collectors, the vacuum-tube collectors work better on cloudy days and cold climates due to both, their ability to collect the diffuse radiation and their very-low heat losses. The vacuum chamber minimizes the convection heat losses as much as the modern low-emissivity coatings minimize the infrared-radiation heat losses, leading to collectors that can heat the refrigerant up to 200 °C (Sabiha et al., 2015). This feature has created new applications for vacuum-tube collectors, like solar adsorption & absorption refrigerators (Zhiqiang, 2005; Zhang et al., 2011) and high-temperature solar cookers (Sharma et al., 2005; Esen, 2004).

The research on how to increase the efficiency of vacuum tubes for solar collectors has continued up today including some new approaches, such as machine learning by using artificial neuronal networks, useful for extracting the knowledge from manufacturer's databases (Liu et al., 2017; Li et al., 2017). These efforts have led to achieving very high yields, but conversely, they have caused more concerns about overheating of the water tank and the stagnation temperature on the vacuum tubes. These behaviors are recognized as the major problems of solar collectors, leading to vaporization and glycol degradation, among other problems (Mercs et al., 2016). As we shall discuss, these improved tubes actually limit the collector's design when it is intended for satisfying the SHWD, that is, for achieving moderate temperatures around 55 °C.

This overheating could lead to reaching very high temperatures and pressures within the water tank (Quiles et al., 2014); it may occur after that the collector runs for several sunny days without water demand, as for example during summer vacations. Most collectors have a single system for dealing with overheating, which consists in discharging hot steam to the atmosphere by opening the pressure-relief valve. However, this solution is forbidden in many developed countries, in which it is unacceptable to waste the water from district grid. In addition, in fact, this unique system should be considered only as a security system and, therefore, not available as a daily control system. Concerns about overheating are probably the main reason why many users are reluctant to use vacuum-tube collectors in their homes. Regarding this issue, some manufacturers now include some controlling actions pursuing to deal with this, for example, a "vacation program" in which the refrigerant is cooled during nights by using an external heat exchanger (Frank et al., 2015). However, this concept is forbidden within the design of most solar collectors, which are just based on passive

E-mail address: juanico@comahue-conicet.gob.ar.

https://doi.org/10.1016/j.solener.2018.07.021
Received 11 February 2018; Received in revised form 1 July 2018; Accepted 7 July 2018

mechanisms. These simplest designs include an upper tank in order to create the free-convection cooling flow between the vacuum tubes and the tank, by using some of these two designs:

(1) The first design uses the simplest kind of tubes (mostly used in temperate or warm climates), in which the refrigerant circulates into the vacuum tubes (so-called the water-in-glass tubes).
(2) The second design uses the heat-pipe tubes, in which their condensers are submerged into the tank.

In both designs are obtained an efficient heat transfer mechanism between the tubes and the tank, and thus, the temperature jump involved is very low. This feature is another advantage of vacuum-tube solar collectors compared to flat solar collectors having a single recirculation loop and so, they obtain a relatively high (up to 40 °C) temperature jump the between the collector and tank (Juanicó et al., 2017; Chen et al., 2015).

Recent researches have been focused in the development of a new glazing with temperature-controlled solar transmittance, which is designed for protecting the flat plastic solar collectors against the damage caused by overheating (Muehling et al., 2014). This solution gives a temperature-dependent reduction of solar transmittance by means of increasing the backscattering of the incident solar radiation (thermotropism). Although these new thermotropic materials have gotten some success (reduction of 28% on the total transmittance), this technology is not useful for vacuum-tube collectors, due to two main reasons:

(1) The thermotropic additive leads to getting a lower transmittance when this mechanism is not working (80%) compared with the standard borosilicate glass (93%). Therefore, this additive would penalize the collector's performance working on low temperatures and during cloudy days.
(2) The manufacturing process includes a lamination step that cannot be easily performed for the cylindrical geometry of tubes.

This first limitation can be overcome by using another approach; here, the solar properties of the absorber are modified by using a smart selective coating that increases strongly its infrared emissivity (the thermochromic effect) above some critical temperature (~70 °C). In this way, some researchers have reduced 36 °C the stagnation temperature of flat solar collectors (Mercs et al., 2016) by using a patented smart coating based on vanadium and aluminum oxides. On the other hand, this coating presents a high solar absorption coefficient (94%) and a low emissivity (6%) for temperatures lower than 70 °C and so, really it does not affect the collector's performance during cloudy days. However and related to the second limitation, up today this novel technology developed at laboratory scale is still not feasible for applying on vacuum tubes, due to the special kind of coating process (by magnetron sputtering) used.

Although both previous works have studied different manners for dealing with the overheating, they both are focused on changing a particular element of the collector and they lack in considering the full thermo-solar behavior of the collector during the overheating process, which must be considered along several days without water demand.

On the other hand, Quiles et al. (2014) have performed a dynamical modeling for forced-convection flat solar collectors. He has shown that for low-quality collectors (that is, having high linear heat-losses coefficient a_1 of 4.5 W/(m^2 K)) are observed tank's temperatures up to 80 °C, which nonetheless are easily reached on the first day without water consumption. On the contrary, for better quality collectors (a_1 ~ 3.5 W/(m^2 K)) and after that several days, the tank temperature can continuously grow up beyond 95 °C. This work has modeled the collector by using an analytical thermal model, which is used for determining the influence of several parameters on the overheating process, such as the type of insulation, the length of piping and the volume of the tank, which are seldom considered in the literature (Juanicó et al., 2017). In this way, this work has contributed to better understanding the main role that the dynamic plays on the overheating, which cannot be considered by just an instantaneous balance of energy or neither as a one-day cycle. However, the weakness of the Quiles's approach consists in precisely to have considered an analytical model, which in turns has forced him to consider a linear approximation for describing the collector's and other heat-losses terms. Although this is a common assumption, in this case, it is not a good approximation. In this work, instead, we have used a fourth-order approximation for the efficiency function, since it allows us to distingue between both physical mechanisms involved, the linear term of convective heat losses and the fourth-order term of infrared radiation heat losses. Hence, we can study one by one the influence of each term on the dynamic behavior of the collector, although, on the other hand, it implies to develop a numerical modeling for performing its temperature evolution.

In this work, we have used a numerical model for studying the dynamical behavior of solar collectors on the most exigent conditions related to overheating and we have determined this condition. After that, we use this most exigent condition for studying two different ways in which we could avoid the overheating, by increasing the convective or infrared-radiation heat losses by means of modifying the vacuum tubes manufacturing process. Finally and by using these modified vacuum tubes, we will study an improved collector assembled with 50 tubes (instead of 20 standard tubes, for a 200 l water tank), showing that this enlarged collector could fully provide the daily demand, even working on cloudy days.

2. Solar-thermal modeling

2.1. Solar modeling

The following equations describe the apparent trajectory of the sun. For cylindrical tubes whose generatrix has a north-south orientation and having diameter D, length L and number of tubes N, its projected normal surface (S_n) is independent of the azimuthal (ψ) solar angle and is only related to the altitude solar angle (α) and the collector's tilt angle (β), by Eq. (1). Here, for an hour (t) of a given day (d), the solar altitude (α) obtained at given latitude (θ) location and having a δ declination angle is calculated going through Eqn. (2)–(8):

$$S_n = NDL\sin(\alpha+\beta) \text{ if } \alpha > 0(\text{day}), \text{ or } S_n = 0 \text{ if} \alpha < 0 \quad (1)$$

$$\delta = 23.45\sin(360°(d-81)/365) \text{ for } d = 1, 2. ..365 \quad (2)$$

$$\psi = 360°(t/24h)-180° \text{ for } 0 < t < 24h \quad (3)$$

$$C_1 = \sin(\theta)\sin(\delta) \quad (4)$$

$$C_2 = \cos(\theta)\cos(\delta) \quad (5)$$

$$S_1 = C_1 + C_2\cos\psi \quad (6)$$

$$S_2 = \sqrt{1-C_1^2} \quad (7)$$

$$\alpha = arc\tan(S_1/S_2) \quad (8)$$

Then, by using the normal area calculated along the day, S_n (t), the solar power absorbed by the collector at any instant, $P_a(t)$, can be calculated from the total solar irradiance, I, and the collector's efficiency, μ (t), as:

$$P_a(t) = IS_n(t)\mu(t) \quad (9)$$

where the total solar irradiance, I, will be assumed as having a constant value along the day, but not having a constant direction, since its direction always follows the apparent trajectory of the sun. In this way, we are defining a total solar irradiance that has the same direction that its direct component, but that has a constant value equal to the sum of the average values of the direct and diffuse radiations. Thus, this constant I value will we calculated as the constant direct solar radiation

that would cause the same daily average irradiation on the earth's surface, and so, in this way this I will be equivalent to the actual solar radiation, which usually has a variable value (and also has a direct and a diffuse variable values) along the day. Therefore, this I value can be calculated directly from solar charts, from which are worldwide available the monthly averages of the total solar irradiation on a level surface (in MJ/m^2/day), but not their direct and diffuse components. This approximation will be accurate during shiny days (when 90% of the actual solar irradiation is the direct irradiation) and worse on cloudy days, but it will be always reasonable for the purpose intended here, which is to describe the temperature evolution of the collector along the day. Let us note that I is not just its normal part to the collecting surface, I_n. The instantaneous efficiency, $\mu(t)$, introduced in Eq. (9) will be calculated in the next section.

2.2. Thermal modeling

The collector has a water tank connected directly to the vacuum tubes, which stored as sensible heat the solar energy absorbed by the vacuum tubes. The balance of energy between the power absorbed (P_a) by the tubes and the power of heat losses (P_l) of the collector's tank to the ambient, determines the temperature evolution of the collectoŕs tank, $T(t)$, being:

$$(M_w Cp_w + M_s Cp_s)(dT/dt) = P_a - P_l \tag{10}$$

where M_w and M_s are the water mass and steel masses of the tank and Cp_w and Cp_s are their heat capacities, respectively. The heat losses within the vacuum tubes must not be considered here, since they have already been included in the efficiency curve, which plots the collector's efficiency as function of the temperature jump between the collector and ambient, T-T_a, and is commonly approximated by its optical efficiency (a_0) and the linear (a_1) and second-order (a_2) heat-losses coefficients, by:

$$\mu = a_0 - \frac{a_1(T-T_a)}{I_n} - \frac{a_2(T-T_a)^2}{I_n} \tag{11}$$

Let us here remark two points. Firstly, it is usually considered that the linear coefficient (a_1) is equivalent to the total heat transmission coefficient (U). Actually, this is true for flat collectors, but considering cylindrical tubes, in which the solar area ($=DL$) is different than the heat loss area ($=\pi DL$), thus $a_1 = \pi\ U$ for tube collectors. Furthermore, since the heat-conduction losses are negligible on vacuum tubes, the U value is similar to the convection coefficient, h. This concept is often overlooked when two coefficients (a_1 and a_2) are used for fitting experimental data, but it will be relevant here because we will modify the convective heat losses, as we shall see in next section. On the other hand, the physical meaning of the quadratic coefficient (a_2) is not so clear as the linear one (a_1) since the other heat losses involved are related to the infrared radiation mechanism, which is well described by a fourth-order (T-T_a)^4 term instead of a quadratic (T-T_a)^2 term. The flux of infrared radiation heat losses on a tube, $q"_{rad}$, can be calculated (Bergman et al., 2011) by:

$$q"_{rad} = (\pi.\ D.\ L)\sigma\varepsilon(T^4 - T_a^4) \tag{12}$$

where σ is the Stefan-Boltzmann's constant and ε is the infrared emissivity of the vacuum-tube absorbing coating. Usually, h and ε have low values ($\sim$0.3 W/m^2 °C and 0.04, respectively) that illustrates the high success of vacuum-tube collectors that can heat up to 200 °C, comparing for example with flat collectors ($h \sim$ 10 W/m^2 °C) that can hardly achieve 100 °C. However, this goal is actually a drawback in order to improve the performance of vacuum-tube collectors for SHWD. Going back to the efficiency function (Eq. (11), we are proposing now to use a fourth-order term instead of the quadratic one, being:

$$\mu = a_0 - \frac{a_1(T-T_a)}{I_n} - \frac{a_4(T-T_a)^4}{I_n} \tag{13}$$

It is interesting to note that we have fitted (by least squares or linear regression) the efficiency curve used for this study (ESTIF, 2006) by using a fourth-order term (Eq. (13) and a quadratic term (Eq. (11), and in both cases we have obtained the same accuracy, according to the fourth-order phenomenon involved.

Let us consider again the energy balance given by Eq. (10). The power of heat losses (P_l) on the tank is calculated considering its external area, A_t, the heat conductivity (k) and thickness (s) of its isolative layer of polyurethane foam (k = 0.029 W/(m K), s = 0.05 m), according to the Fourier's heat-conduction law:

$$P_l = kA_t\frac{(T-T_a)}{s} \tag{14}$$

From here, the Eq. (10) can be numerically solved by integrating the temperature rate (dT/dt) along the n time step by using the simplest explicit scheme (the Euler's approximation) by:

$$(M_w Cp_w + M_s Cp_s)(dT/dt) \cong (M_w Cp_w + M_s Cp_s)\frac{(T^n - T^{n-1})}{\Delta t} = P_a^n - P_l^n \tag{15}$$

Thus, the temperature value in the present (n) time step, T^n, can be calculated from all magnitudes known on this time step and the temperature value known at the previous time step, T^{n-1}. In this way, the daily evolution can be calculated by following an iterative process that starts with an initial value, T_i. Finally, the ambient temperature evolution is modeled as usual by using a cosine curve (Chen and Liu, 2004):

$$T_a(t) = T_a^* + \Delta T_a \cos[\pi(t-14)/12] \tag{16}$$

2.3. Numerical modeling

The fully solar-thermal modeling described by previous Eqs. (1)–(16) can be easily programmed in a spreadsheet (see Supplementary Material). Considering that the temperature varies slowly along the day, a relatively large time step can be used (Δt = 0.1 h) and it still provides accurate results. This assumption was checked by taking a time step ten times smaller (0.01 h) and verifying that the error obtained was smaller than 2%. Therefore, this numerical tool is useful to study thermally any vacuum-tube solar collector working on any condition, which is defined by this set of parameters:

(1) Climatic conditions: latitude, θ, date of the year, d, total solar irradiation flux, I, mean ambient temperature, T_a^*, and amplitude ambient temperature, ΔT_a;
(2) Collecting geometry: collector's tilt angle, β; diameter, length and number of tubes, D, L and N;
(3) Efficiency curve parameters: a_0, a_1, a_4.
(4) Tank parameters: water mass, M_w, steel mass, M_s, external area, A_t, and insulation thickness, s.

Supplementary data associated with this article can be found, in the online version, at https://doi.org/10.1016/j.solener.2018.07.021.

After setting all these parameters and the physical properties (k, Cp_w, Cp_s), the first module of the spreadsheet (columns A to E) calculates the apparent daily sun trajectory. From here, we calculate the projected collector's area (S_n) normal to the sun rays (column F) and the solar power irradiated onto the collector's tubes (P_i), being $P_i = S_n\ I$ (column G). The evolution of the ambient temperature (column H) together with the previous tank temperature (T^{n-1}) are used for calculating the collector's efficiency, μ^n (column I). Thus, the absorbed power (P_a^n) is calculated (column J) by multiplying the irradiation power (P_i^n) and the efficiency. On the other hand, the tank heat losses (P_l^n) is calculated from the temperature jump between the previous temperature and the current ambient temperature (T^{n-1}-T_a^n) in column K. Finally, the current tank temperature (T^n) is calculated from the energy balance (Eq. (15). In this way and repeating iteratively this

procedure, we can obtain the daily evolution of the tank temperature. Here, we could have used a "clock cycle" (0–24 h), but instead, we will consider a sun cycle (from the sunrise to the next sunrise), which is more suitable for representing the daily cycle composed for the heating process during the morning and the nocturnal cooling. However, programming this sun cycle can be cumbersome on a spreadsheet framework considering that the sunrise time is variable along the year. We solve this trouble by selecting an annual average cycle (from 6 a.m. to 6 a.m.) that is exact at both equinoxes and besides, it minimizes the error in other dates; this error was verified to be always lower than 2%. Finally, after calculating the daily temperature evolution in this manner, some general results can be obtained. Hence, the total energy irradiated (E_i), the total energy absorbed (E_a) by the collector, and the total energy lost by the tank (E_l) are all calculated by integrating the G, J and K columns, respectively. Then, the average collector's efficiency is obtained as $= E_a/E_i$, and similarly does the average tank's efficiency, as $= 1 - E_l/E_a$. Two other interesting values calculated are the maximum temperature of the tank and its temperature at sunrise. In this work, the collector's efficiency curve considered is defined by their parameters: $a_0 = 0.758$, $a_1 = 1.53$ and $a_4 = 4.8 \cdot 10^{-7}$, which represent a standard curve for evacuated tubes according to the European Solar Thermal Industry Federation (ESTIF, 2006). We will study a solar collector that uses 20 of these tubes and has a 200-l water tank built with a 5 cm-thickness insulation layer.

3. Results

3.1. Sensitivity analysis of the collector's tilt angle for overheating limitation

We study now the influence of the collector's tilt angle on the overheating behavior, considering that it could be useful for limiting this phenomenon. Firstly, we will consider a maritime temperate location (Buenos Aires, 35° south latitude, which must be set as −35° in our spreadsheet code) whose climatic conditions are: $T_a = 30\,°C \pm 5\,°C$ during summer, and $T_a = 15\,°C \pm 5\,°C$ during winter. The maximum temperature achieved during a summer day ($d = 1$) and a winter day ($d = 180$) are shown in Tables 1 and 2 for four different tilt angles: $\beta = 25°, 45°, 60°$ and 90° (vertical), starting with an initial temperature equals to the mean ambient temperature (30 °C in summer and 15 °C in winter). Table 2 shows that the vertical collector gets a better winter performance that the collector using the recommended angle (45°), and besides it achieves a remarkable lower maximum temperature (66 °C vs. 84 °C) in summer (see Table 1), which otherwise does not compromise its performance for providing sanitary hot water.

Hence, and encouraged by these promising results, we will study now the peak of overheating that it would reach on a high-requirement condition (like summer vacations), for which there is no water demand and having a high solar irradiation ($I = 800\,W/m^2$). This condition can be simulated on our numerical model by calculating the evolution of the first day and after that, by calculating the second day by substituting the initial temperature (cell B17) with the final temperature achieved in the first-day cycle (cell L269), and repeating this iterative process along several days until the collector reaches its periodic steady-state regime. Table 3 shows the peak temperature obtained in this way and the number of daily cycles needed to reach the 131 °C level, which is the highest boiling point of the glycol solution (Homepower Magazine, 2017). Here we can show that the vertical position cannot eliminate the overheating, although the 131 °C level is reached just after seven days (see Fig. 1). On the contrary, the collector suffers high temperatures and quickly exceeds the 131 °C level when it is installed on lower tilt angles, being $\beta = 45°$the worst case.

Table 1
Maximum temperatures (one-day cycle) for different tilt angles and solar fluxes in summer ($d = 1$).

I (W/m^2)	$\beta = 90°$	$\beta = 60°$	$\beta = 45°$	$\beta = 25°$
800	66	82	84	82
600	57	69	71	69
400	49	56	58	56
200	40	43	44	44

Table 2
Maximum temperatures (one-day cycle) for different tilt angles and solar flux in winter ($d = 180$).

I (W/m^2)	$\beta = 90°$	$\beta = 60°$	$\beta = 45°$	$\beta = 25°$
800	60	62	58	49
600	49	50	47	41
400	38	39	37	32
200	27	27	26	26

Table 3
Peak temperature and the number of days to reach 131 °C (summer vacations).

$\beta = 90°$		$\beta = 60°$		$\beta = 45°$		$\beta = 25°$	
137 °C	7 days	164 °C	3 days	168 °C	2 days	165 °C	3 days

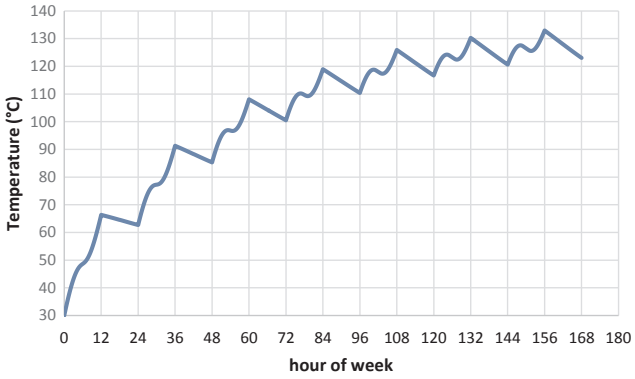

Fig. 1. Temperature evolution of collector on vertical position in summer vacations.

The previous sensitivity analysis is repeated now for both, a warm location at the Equator's line ($\theta = 0°$, $T_a = 35\,°C \pm 5\,°C$ in summer and $T_a = 20\,°C \pm 5\,°C$ in winter) and a cold high-latitude location ($\theta = -50°$, $T_a = 30\,°C \pm 5\,°C$ for summer and $T_a = -5°C \pm 5\,°C$ in winter). These results are summarized in Tables 4 and 5, in which the last row shows the peak temperature achieved during the summer vacation ($I = 800\,W/m^2$) condition. Here we observe again that the vertical position helps us to reduce the peak of temperature, but this is not enough to avoid the overheating, even in the cold high-latitude location. Besides, we can observe another interesting result. The 45° tilt angle always gets the hottest peak temperature within the wide range of latitudes studied and therefore, following a conservative approach, we will use this angle in next analyzes. On these analyzes, we will study two proposals for self-limiting the peak temperature so that the

Table 4
Maximum temperatures (one-day cycle) for different tilt angles during summer/winter conditions in the Equator's location.

I (W/m^2)	$\beta = 90°$	$\beta = 60°$	$\beta = 45°$	$\beta = 25°$
800	78/63	89/74	89/74	84/69
600	67/52	75/60	76/61	72/57
400	62/42	62/47	62/47	60/45
200	49/31	49/34	49/34	48/33
Peak	148	166	167	160

Table 5
Maximum temperatures (one-day cycle) for different tilt angles during summer/winter conditions in the 50° latitude location.

I (W/m^2)	β = 90°	β = 60°	β = 45°	β = 25°
800	71/46	84/45	86/40	83/31
600	61/37	71/36	72/32	70/25
400	51/27	58/27	58/24	57/20
200	41/18	44/17	45/16	44/14
Peak	133	155	157	152

collector can avoid the concerns about the tanks overheating.

3.2. First proposal: modifying the convective heat losses of vacuum tubes

This proposal consists of increasing the convective heat losses, which is modeled by increasing the a_1 coefficient of efficiency (Eq. (13). The collector's manufacturer can easily perform this proposal by just increasing the air pressure inside vacuum tubes and so, adjusting the value of a_1. So, let us calculate the a_1 value necessary for getting two different peak temperatures during a summer vacation period: (1) 111 °C and (2) 131 °C. Here, the lower (111 °C) temperature is related to the simplest water-in-glass vacuum tubes usually used in temperate and warm climates for which the water pressure must keep down 0.5 bar above the atmospheric pressure. The higher level (131 °C) represents the highest breakdown temperature of antifreeze liquids used on cold climates, and it is the maximum temperature for a water-saturated (2 bar) tank. These conditions are both related to heat-pipe tubes, the first one when an antifreeze circuit is used, and the second one when an upper water tank is used, regarding that the relief valve is usually set to a higher (3 bar) level. Therefore and by considering both more exigent conditions, the climatic (latitude 0°) and the collector's tilt angle (45°), we calculate now the a_1 levels needed for avoiding the collector overheating by using the iterative process explained before, obtaining a_1 = 6.1 W/m^2 °C (for 111 °C) and a_1 = 4.2 W/m^2 °C (for 131 °C). At this point, let us remark the advantage of the dynamic modeling developed. The a_1 value could also be determined by just clearing it from matching the efficiency to zero in Eq. (13) (μ = 0), that would lead to a_1 = 5.9 W/m^2 °C for the 131 °C level. Therefore, in this way we had obtained an overestimated a_1 value, due to not have considered the tank losses and the collector's dynamic behavior. Moreover, in this way, we cannot determine the number of days needed to reach the periodic stationary.

On the other hand, and now by using our numerical dynamical model with a_1 = 4.2 W/m^2 °C, we observe that the collector reaches its period regimen only after ten fully sunshine days and without exceeds the peak level (131 °C), going to the 120–130 °C range during the periodic regimen. Besides, other analyzes can be performed, such as considering, for example, one raining day (I = 50 W/m^2) within a full shiny week and recalculating the temperature evolution after this very cloudy day, so determining the number of sunshine days that the system needs in order to reach again a dangerous peak temperature.

Let us study now how these modified vacuum tubes (increasing their convective heat losses) penalize the collector performance when it works in winter. Table 6 shows the maximum temperature (T_m) and the maximum temperature jump (T_m-T_i) achieved by both, the modified and the original collectors, for the same three locations previously studied, and for the worst case (β = 45° and I = 800 W/m^2). Here, we can observe that for vacuum tubes having the lower heat losses (a_1 = 4.2 W/m^2 °C), the penalization of performance is between 9% and 15%, meanwhile, this penalization increases up to 26% for the tubes having the higher heat losses (a_1 = 6.1 W/m^2 °C). Fig. 2 illustrates the curve of efficiency vs. (T-T_a) on I = 800 W/m^2, which is obtained for these three different tubes. Here we observe that the performance of both modified collectors is noticeably lower than the original one. Summarizing, this solution for the overheating (by increasing the convective heat losses) has a marked drawback on the collector's performance during winter.

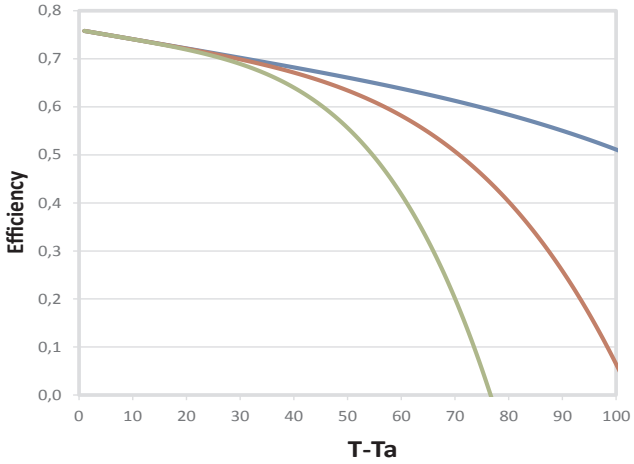

Fig. 2. Efficiency curve for three collectors (a_1 = 1.53, 4.2 or 6.1 W/m^2 °C) for I = 800 W/m^2.

3.3. Second proposal: modifying the emissivity of vacuum tubes

The second proposal consists in increasing the infrared emissivity of vacuum tubes in order to increase the heat losses by infrared radiation, which implies a larger a_4 value in the collector's efficiency equation (Eq. (13)). The collector's manufacturer could make this change by using "old-fashion" sensitivity coatings or by using other new techniques (Mercs et al., 2016). The a_4 values calculated by our model for limiting the maximum temperature are: (1) $a_4 = 4.3{\cdot}10^{-6}$ W/m^2 °C^4 (for 131 °C) and (2) $a_4 = 1.5{\cdot}10^{-5}$ W/m^2 °C^4 (for 111 °C), always using the original value of convective heat losses (a_1 = 1.53 W/m^2 °C). Table 7 shows the winter performance for these both cases. Here we can observe that the collector's performance is not penalized within the range of low temperatures (that is, its winter performance) and it is barely penalized in the medium temperature range, which is also reflected by their efficiency curves illustrated in Fig. 3. Therefore, these modified collectors have similar ability than the original for satisfying the SHWD, but meanwhile, they can avoid concerns about overheating. This feature opens a new dimension of design, useful for creating an enhanced collector what could fulfill the SHWD even running on low solar resources.

Table 6
Maximum temperature/maximum temperature jump for the original and modified a_1 values on winter and for I = 800 W/m^2 on three locations studied (Tables 1–5) and β = 45°.

a_1 (W/m^2 °C)	θ = 0° $T_m/\Delta T_m$	θ = 35° $T_m/\Delta T_m$	θ = 50° $T_m/\Delta T_m$
1.53	74/39	58/43	40/30
4.2	68/33	54/39	36/26
6.1	64/29	52/37	33/23

Table 7
Maximum temperature/maximum temperature jump for the original and modified a_4 values on winter and for I = 800 W/m^2 on the three locations previously studied (Tables 1–5) and β = 45°.

a_4 (W/m^2 °C^4)	θ = 0° $T_m/\Delta T_m$	θ = 35° $T_m/\Delta T_m$	θ = 50° $T_m/\Delta T_m$
$4.8{\cdot}10^{-7}$	74/54	58/38	40/30
$4.3{\cdot}10^{-6}$	73/53	58/38	40/30
$1.5{\cdot}10^{-5}$	72/52	58/38	40/30

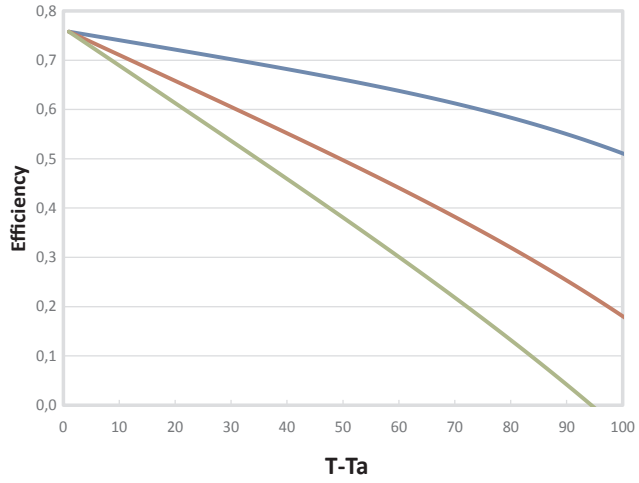

Fig. 3. Efficiency curves modifying the collector's emissivity ($a_4 = 4.8 \cdot 10^{-7}$, $4.3 \cdot 10^{-6}$, $1.5 \cdot 10^{-5}$ W/m^2 °C^4) for $I = 800$ W/m^2.

3.4. Enhanced collector by using a greater number of modified tubes

We will study the performance of a new collector, which is assembled by using a greater number of vacuum tubes (having modified emissivity as we have discussed in the previous subsection) in order to better satisfy the SHWD working on low solar resources. Let us remark that on the contrary, this choice is absolutely forbidden by using the state-of-the-art technology of vacuum tubes since it could lead to a dangerous overheating. For example, if the number of vacuum tubes was doubled (40), the collector would reach 128 °C every sunny day in the temperate climate of Buenos Aires and so it would need to open daily the pressure relief valve. Moreover, if this action fails, then the collector would reach 184 °C, which would cause an extremely dangerous overpressure (10 bar) in the water tank. This example is useful for illustrating how strongly the overheating actually limits the number of vacuum tubes used in most standard collectors, which in turns reduces their performance on cloudy days.

Regarding the sensitivity analysis of the number of vacuum tubes, we will consider now two kinds of climates and vacuum-tube technologies. The simplest (water-in-glass) tube is commonly used on temperate and warm climates, and so the lower peak temperature (111 °C) will be considered (that is, using low-modified tubes having $a_4 = 1.5 \cdot 10^{-5}$ W/m^2 °C^4). On the other hand, the heat-pipe tubes are suitable for cold climates and so, the higher peak temperature (131 °C) will be considered (that is, using high-modified tubes having $a_4 = 4.3 \cdot 10^{-6}$ W/m^2 °C^4) for this case. Table 8 shows the winter performance for the low-modified collector by using different numbers of vacuum tubes and working in the temperate climate of Buenos Aires on its best tilt angle ($\beta = 60°$, which enhances the winter performance). Here we can observe that the 20-tube collector can fulfill the SHWD only having solar resources around 600 W/m^2, and on the contrary, we observe that a solar resource of just 200 W/m^2 is enough good for the 50-tube collector. Although a very-cloudy day actually would imply to consider a lower solar flux ($\sim$100 W/m^2), let us remark the well-known ability of vacuum tubes for collecting the diffuse radiation. Therefore

Table 8
The maximum temperature in winter for different numbers of tubes, $\beta = 60°$, $\theta = 50°$, $a_4 = 1.5 \cdot 10^{-5}$.

I (W/m^2)	$N = 20$	$N = 30$	$N = 40$	$N = 50$
800	61	78	87	91
600	50	64	75	81
400	39	49	58	65
200	26	33	38	42

Table 9
The maximum temperature in winter for different numbers of tubes, $\beta = 80°$, $\theta = 50°$, $a_4 = 4.3 \cdot 10^{-6}$.

I (W/m^2)	$N = 20$	$N = 40$	$N = 60$	$N = 100$
800	47	76	92	100
600	37	61	77	89
400	28	44	57	72
200	18	26	32	43

and for considering the thermal performance studied here, it is reasonable to assume that a diffuse 100 W/m^2 solar irradiation produce an equivalent yield to a direct 200 W/m^2 solar irradiation.

On the other hand, the winter performance for the cold location (50°, $T_a = -5$°C $\pm$ 5 °C) is presented in Table 9 by considering its best tilt angle ($\beta = 80°$) and by using the high-modified tubes ($a_4 = 1.5 \cdot 10^{-5}$ W/m^2 °C^4). Here, we note that the 20-tube collector needs a very high ($I = 800$ W/m^2) solar irradiation to fulfill the SHWD, but using 40 tubes this goal can be achieved on average solar resources (400 W/m^2). For cloudy days, using 60 tubes can achieve the SHWD partially or it can be fulfilled by using 100 tubes. In this last choice, we can also observe how our overheating-limitation design works; the maximum temperature achieved on a fully sunshine (I = 800 W/m^2) day (100 °C) is barely higher than by using a 60-tubes collector (92 °C) due to their high infrared-radiation heat losses. This behavior can also be observed by considering the average collector's efficiency (cell F15 in the Suppl. Mat.). For example, following the first row of Table 9 with $I = 800$ W/m^2, collectors having 20, 40, 60 and 100 tubes lead to average efficiencies of 69%, 62%, 52% and 34%, respectively, showing that the efficiency is markedly reduced as much as the working temperature is increased. Whether the original collector (having tubes with $a_4 = 4.8 \cdot 10^{-7}$) had been considered, for example with 100 tubes, the maximum temperature achieved would be 145 °C.

4. Conclusions

In this paper is developed a full solar-thermal modeling of solar collectors that comprises a fourth-order modeling of vacuum tubes, which are numerically performed on a spreadsheet. This numerical tool has demonstrated to be useful for representing the nonlinear dynamics of solar collectors, which has many coupled parameters, especially for the vacuum-tube phenomena involved. We have demonstrated that a fourth-order model for the efficiency function of the tubes (instead of the linear and quadratic models that are often used) is the right tool for representing the different kinds of heat losses (by convection and by infrared radiation) in a comprehensive physical manner, which allows us to study each one on one.

We have shown that the scenario in which solar collectors have to work is challenging. Solar collectors have to work with an intrinsically variable solar resource and have to fulfill an exigent daily demand during winter as well as dealing with dangerous overheating during summer vacations. Hence, it is necessary to study the dynamical response of the system during several days for understanding these opposite-trend processes. Concerns about overheating actually limit the number of vacuum tubes used for a given tank size and on the contrary, a higher number of tubes is desirable for improving their winter performances. However, since there is not currently any physical solution to control the overheating, an increasing of the number of vacuum tubes could lead to dangerous conditions. Therefore, solar collectors must be designed by following a compromise solution, in which its winter performance is strongly penalized in order to reduce the overheating concerns, although otherwise not completely solving this trouble.

On the other hand, the technology of vacuum tubes is evolving to better quality ones having lower both, infrared radiation and air

convective heat losses, in order to heat up to 200 °C. However, as it was discussed, convective losses should be further reduced as much as radiative losses should be actually increased by going a step back in the technology of selective coatings. By using our modeling, we can calculate the exact relation needed between both kinds of heat losses in order to avoid intrinsically the overheating and simultaneously not penalizing the collector's performance when it works in average temperatures. This new feature has opened a new choice for designing a solar collector that could fulfill the daily SHWD working on all climatic conditions. We have found that this goal can be reached in temperate and warm climates by doubling the number of tubes, but this is more difficult to achieve in cold climates.

The previous values calculated by using average-quality vacuum tubes can be slightly decreased by using tubes of the best quality. Beyond this, we have redefined at all the concept of best-quality tubes. Next, it will be relevant to achieve new vacuum tubes having lower convective heat losses, but either not having a lower emissivity.

Finally, we expect that the understanding of the dynamical response of solar collectors presented here can help to create other new design solutions. We could essay now, for example, a new modified tank, in which the bottom hemisphere of the cylindrical annular cavity between both tanks (the internal stainless steel one containing the water and the external one containing the isolative foam) is empty and black painted. In this way, the infrared-radiation heat losses are increased when the tank achieves high temperatures, as much as the air-convective heat losses are negligible during winter nights since the upper water tank is hotter than the lower external tank and so, the air free-convection heat transfer through the air gap is avoided.

Acknowledgements

This work was supported by the project CONICET PIP "Uso eficiente de energía y aprovechamiento del recurso solar en la Patagonia Andina".

References

Bergman, T., Lavine, A., Incropera, F., DeWitt, D., 2011. Fundamentals of Heat and Mass Transfer, 7th ed., John Wiley & Sons, ISBN 978-0470917855.

Chen, G., Doroshenko, A., Koltun, P., Shestopalov, K., 2015. Comparative field experimental investigations of different flat plate solar collectors. Sol, Energy 115, 577–588.

Chen, W., Liu, W., 2004. Numerical and experimental analysis of convection heat transfer in passive solar heating room with greenhouse and heat storage. Sol. Energy 76, 623–633.

Esen, Mehmet, 2004. Thermal performance of a solar cooker integrated vacuum-tube collector with heat pipes containing different refrigerants. Sol. Energy 76, 751–757.

ESTIF (European Solar Thermal Industry Federation). 2006. Adapted from a spreadsheet by Jan Erik Nielsen. < http://solarprofessional.com/sites/default/files/articles/ajax/docs/6_SP2_6_pg58_Stickney-8.jpg > .

Frank, E., Mauthner, F., Fischer, S. 2015. Overheating prevention and stagnation handling in solar process heat applications. IEA Solar Heating&Cooling Programme Task 49. Available in: < http://task49.iea-shc.org/Data/Sites/7/frank_iea_shc_task49_overheatingstagnationreport_approved_v-2-3.pdf > .

Homepower Magazine, 2017. < https://www.homepower.com/articles/solar-water-heating/domestic-hot-water/overcoming-overheating > .

Juanicó, L.E., Di Lalla, N., González, A.D., 2017. Full thermal-hydraulic and solar modeling to study low-cost solar collectors based on a single long LDPE hose. Renew. Sustain. Energy Rev. 73, 187–195.

Liu, Z., Li, H., Liu, K., Yu, H., Cheng, K., 2017. Design of high-performance water-in-glass evacuated tube solar water heaters by a high-throughput screening based on machine learning: a combined modeling and experimental study. Sol. Energy 142, 61–67.

Li, H., Liu, Z., Liu, K., Zang, Z., 2017. Predictive Power of Machine Learning for Optimizing Solar Water Heater Performance: The Potential Application of High-Throughput Screening. Int. J. of Photoenergy, Hindawi Ed., ID 4194251, 10 pages, 10.1155/2017/4194251.

Mercs, D., Didelot, A., Capon, F., Pierson, J.F., Hafner, B., Pazidis, A., Föste, S., Reineke-Koch, R., 2016. Innovative smart selective coating to avoid overheating in highly efficient thermal solar collectors. Energy Proc. 91, 84–93.

Muehling, O., Seeboth, A., Ruhmann, R., Eberhardt, V., Byker, H., Anderson, C.D., De Jong, S., 2014. Solar collector cover with temperature-controlled solar light transmittance. Energy Proc. 48, 163–171.

Quiles, P., Aguilar, F., Aledo, S., 2014. Analysis of the overheating and stagnation problems of solar thermal installations. Energy Proc. 48, 172–180.

Sabiha, M.A., Saidur, R., Mekhilef, S., Mahian, O., 2015. Progress and latest developments of evacuated tube solar collectors. Renew. Sustain. Energy Rev. 51, 1038–1054.

Sharma, S.D., Iwata, T., Kitano, H., Sagara, K., 2005. Thermal performance of a solar cooker based on an evacuated tube solar collector with a PCM storage unit. Sol. Energy 78, 416–426.

Zhang, G., Wang, D.C., Zhang, J.P., Han, Y.P., Sun, W., 2011. Simulation of operating characteristics of the silica gel–water adsorption chiller powered by solar energy. Sol. Energy 85 (7), 1469–1478.

Zhiqiang, Y., 2005. Development of solar thermal systems in China. Sol. Energy Mater. Sol. Cells 86 (3), 427–442.